THE JOURNAL OF PHYSICAL CHEMISTRY C

Article

Cite This: J. Phys. Chem. C 2019, 123, 9993−9999

pubs.acs.org/JPCC

In Situ Studies on Temperature-Dependent Photocatalytic Reactions of Methanol on TiO_2(110)

Ruidan Zhang,[†,‡,⊥] Haochen Wang,[‡,⊥] Xingxing Peng,[†,‡] Ran-ran Feng,[†,§] An-an Liu,[†] Qing Guo,[‡] Chuanyao Zhou,[‡] Zhibo Ma,*[,‡] Xueming Yang,[‡,∥] Ying Jiang,[†] and Zefeng Ren*[,†,‡]

[†]International Center for Quantum Materials (ICQM) and School of Physics, Peking University, 5 Yiheyuan Road, Beijing 100871, P. R. China

[‡]State Key Laboratory of Molecular Reaction Dynamics, Dalian Institute of Chemical Physics, Chinese Academy of Sciences, 457 Zhongshan Road, Dalian 116023, Liaoning, P. R. China

[§]Key Laboratory of Microgravity (National Microgravity Laboratory), Beijing Key Laboratory of Engineered Construction and Mechanobiology, Institute of Mechanics, Chinese Academy of Sciences, Beijing 100190, China

[∥]Department of Chemistry, Southern University of Science and Technology, 1088 Xueyuan Road, Shenzhen 518055, Guangdong, P. R. China

ABSTRACT: We studied the photocatalytic reaction of methanol on the TiO_2(110) surface in situ by surface sum frequency generation vibrational spectroscopy. The in situ vibrational spectra of the photo-oxidation product, formaldehyde and methyl formate, on TiO_2(110) was unambiguously assigned and identified. The temperature-dependent photocatalytic reaction efficiency was observed and suggested that the thermal diffusion might be important for the photocatalytic reaction. Scanning tunneling microscopy combined with ultraviolet light was used to investigate the photocatalytic reaction efficiency on the hydroxylated TiO_2(110) surface, which shows that the neighboring hydroxyl group on the bridge-bonded oxygen site dramatically inhibits the photo-oxidation of methanol because of the repulsion between hydroxyl groups. Our results provide direct vibrational spectral evidence of photo-oxidation products of methanol on TiO_2(110), show the importance of thermal processes in surface photocatalytic reactions, and deepen our understanding on photochemistry on this surface.

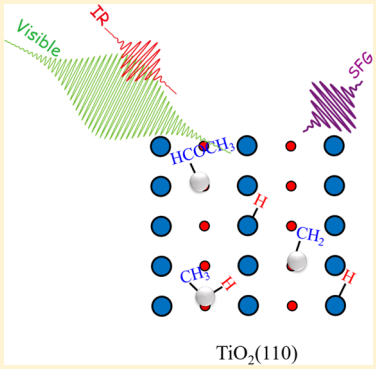

1. INTRODUCTION

Titanium dioxide, TiO_2, has attracted great interest because of its promising application in photocatalytic splitting of water, photodegradation of environmental pollutants, surface superwetting, and so on.[1−7] Methanol, as a simplest alcohol, is often used in benchmark studies of the photocatalytic mechanism on TiO_2 for explanation of oxide surface properties.[8−15] In addition, methanol, as a hole scavenger, can dramatically enhance the photocatalytic activity to split water to hydrogen.[16−20] In the last decade, numerous studies have been carried out on the prototypical model of the photocatalytic reaction of methanol on the rutile TiO_2(110) surface.[14,21−26] However, the mechanism of photocatalytic processes on TiO_2 has not been satisfied to date, especially in the atomic and molecular level.

It is well known that in thermal chemistry, the most active site on TiO_2(110) is the bridge-bonded oxygen (O_b) vacancy site. Alcohol molecules adsorb on the O_b vacancy site and spontaneously dissociate to form the alkoxyl and the hydroxyl (OH_b) groups.[3,5,11] The recombination of OH_b to form water can happen at about 450 K,[8] which competes with the formation of molecular hydrogen.[27] The most abundant photocatalytic reactions occur on the five-coordinated Ti site (Ti_{5c}).[6,21,22] The mixed adsorption structure of molecular and dissociated methanol on Ti_{5c} sites was provided recently by surface sum frequency generation vibrational spectroscopy (SFG-VS), and it was also found that the percentage of the dissociated methanol in the first layer decreases as the coverage increases to more than one layer.[28] The stepwise photo-oxidation of methanol to formaldehyde and further to methyl formate on TiO_2(110) was observed.[24−26]

Temperature-programmed desorption (TPD) is the most commonly used method and a powerful tool to study the mechanism of CH_3OH/TiO_2(110) photocatalytic reaction, especially together with ultraviolet (UV) light sources and intense UV lasers, as reported in the last decade.[21−27,29] However, TPD probes the species desorbing from the surface, which sometimes could be from the reaction during the heating process of the substrate. X-ray photoelectron spectroscopy has also been used to identify the photocatalytic product of methanol on TiO_2(110).[25] To determine the chemical nature of surfaces and adsorbates, the surface vibrational spectroscopy has gained wide recognition for its ability,[30] such as reflection−absorption infrared spectroscopy.

Received: March 10, 2019
Revised: March 25, 2019
Published: March 26, 2019

DOI: 10.1021/acs.jpcc.9b02244
J. Phys. Chem. C 2019, 123, 9993−9999

However, it is difficult to obtain the vibrational spectra on oxides because of the absence of an image dipole and strongly reduced reflectivity.[31]

In this study, we used surface SFG-VS to obtain the vibrational spectra in the C−H stretching range of photocatalytic products of methanol on TiO_2(110). The SFG spectra clearly shows the vibrational features from formaldehyde and methyl formate on TiO_2(110). We also compared the photocatalytic reaction efficiencies at substrate temperature of 120 and 180 K. Our results suggested that thermal processes of methanol and photocatalytic reaction products or the repulsion from OH_b could limit the reaction rate. To elucidate the effect from OH_b, scanning tunneling microscopy (STM) combined with UV light was employed to investigate the photodissociation of methanol on the hydroxylated TiO_2(110) surface.

2. EXPERIMENTAL DETAILS

All SFG measurements were conducted in a compact high pressure/ultrahigh vacuum (UHV) chamber, which is described in detail elsewhere.[32] Commercial rutile TiO_2(110) single crystal (Princeton Scientific) was at 45° with the crystal orientation [001] relative to the plane of light incidence. Sample preparation was done by cycles of 500 eV Ar^+ ion sputtering and vacuum annealing at 850 K. Methanol (99.95% purity) was further purified by several freeze−pump−thaw cycles before the experiment. Almost one layer coverage of methanol was prepared by overdosing methanol at 120 K and subsequent flashing of the substrate at 216 K.[8]

The optical system of SFG-VS has been described elsewhere.[28] The regenerative amplifier (Spitfire Ace, Spectra-Physics) generated 35 fs pulses with 5 mJ per pulse at a 1 kHz repetition rate at the central wavelength of 800 nm. About 3 mJ was used to pump an optical parametric amplifier (TOPAS-C, Light Conversion) and a noncollinear difference frequency generator (NDFG1, Light Conversion), which delivered a tunable IR (2.6−9 μm) in a silver gallium disulfide ($AgGaS_2$) crystal. The central wavelength used in this work was about 3.4 μm with an apparent spectral bandwidth of about 300 cm^{-1} full-width at half-maximum (fwhm). 20 mW of IR measured before the CaF_2 window on the UHV chamber was used in our measurements. About 1 mJ of 800 nm pulses was spectrally narrowed as the visible light (VIS) by using a pulse shaper (1800 l/mm pulse compression grating, Spectrogon; cylindrical lens with 200 mm focal length), normally 4.5 cm^{-1} fwhm and 7.5 mW. The residual 1 mJ was used to generate second harmonic UV light at 400 nm. UV light (4 mW) was soft-focused to about 1.5 mm diameter on TiO_2(110). The IR and VIS pulses were temporally and spatially overlapped on the surface, and the reflected broadband SFG signal was dispersed by a monochromator and then detected by an electron-multiplying charge-coupled device (Princeton Instrument). The incidence angles of SFG, VIS, and IR were 47.9°, 45°, and 57°, respectively. Both polarizations of the VIS and IR were controlled by true zero-order half-wave plates, and the SFG signal polarization was selected and controlled by the combination of an achromatic half-wave plate and a Glan polarizer. The measured SFG spectra were normalized to the SFG signal of ppp (referring to p-polarized SF output, p-polarized visible input, and p-polarized IR input, respectively) polarization combination on the bare TiO_2(110) surface obtained by flashing the sample to 700 K in UHV.

STM experiments were performed in an UHV chamber equipped with a low-temperature STM (Omicron, MATRIX). The vacuum system was baked out for more than 100 h to reduce the residual water to get a base pressure better than 3.5 × 10^{-11} mbar. The TiO_2(110) sample (Princeton, 5 mm × 10 mm × 2 mm) was prepared by multiple cycles of sputtering in 1000 eV Ar^+ ions for 10 min and annealing at ∼900 K for 30 min. During annealing, the sample was mounted on a standard Omicron sample Ta plate holder and heated with a pyrolytic boron nitride heater located behind the sample plate. After this procedure, the concentration of oxygen vacancy was about 10%. The sample was cooled down to 80 K on the stage of the STM scanner which is mounted under a liquid nitrogen dewar. An electrochemically etched tungsten tip was used and all the images were obtained using the constant current mode with a tunneling voltage of 1.25 V and a tunneling current of 100 pA. All the STM images were processed using SPIP software (Image Metrology). As reactants, water and methanol (Sigma-Aldrich) were purified by several freeze−thaw−freeze cycles to remove existing impurities using liquid nitrogen. The molecules were dosed in situ onto the TiO_2(110) surface through a retractable and calibrated doser with a pinhole, and the distance between the sample and pinhole was about 4 cm. This method can minimize contamination of the UHV system. During dosing and laser irradiation, the tip was retracted about 20 μm from the sample to avoid the shadowing effect. The third-harmonic (355 nm) output of a 1064 nm Q-switched HIPPO laser (Spectra-Physics) was used in our experiments, which had a duration of about 12 ns and a high repetition of 50 kHz. The TiO_2(110) sample was illuminated by the laser with an incident angle about 27° through a viewport on the chamber. The beam diameter of laser was ∼5 mm and laser power from 20 to 200 mW was used. After laser irradiation, the increase of sample's temperature was less than 2 K.

3. RESULTS AND DISCUSSION

3.1. Temperature-Dependent Photocatalytic Reactivity of Methanol on TiO_2(110) by SFG Studies. Figure 1 shows the SFG vibrational spectra of methanol with one monolayer coverage on the TiO_2(110) surface before and after different 400 nm UV irradiation durations. All the SFG spectra were taken at the substrate temperature of 120 K, and the substrate was kept at 120 K when it was irradiated by UV light. The spectra show complicated features, including symmetric stretching, ν_s, Fermi resonance, and antisymmetric stretching from both dissociative adsorbed methanol (methoxy, CH_3O-Ti_{5c}) and molecular adsorbed methanol (CH_3OH-Ti_{5c}) at Ti_{5c} sites. Recently, we have successfully assigned these spectra in this C−H stretching region by means of SFG polarization-dependent, methanol coverage-dependent, and UV irradiation treatments.[33] The features at 2806 and 2841 cm^{-1} are assigned to CH_3 symmetric stretching modes from methoxy and molecular-adsorbed methanol at Ti_{5c}, respectively. The Fermi resonances and CH_3 antisymmetric stretching of these two species are highly overlapped in the range from 2887 to 3000 cm^{-1}. The ssp (referring to s-polarized SF output, s-polarized visible input, and p-polarized IR input, respectively) SFG spectra in Figure 1a show that the methoxy peak (indicated by the blue dashed line) decreases with the UV irradiation time, whereas the peak for methanol (indicated by red dashed line) seems the same but broader. Even after further 5 min of UV irradiation, methoxy only decrease a little. It seems the reaction almost stops. The ppp SFG spectra in Figure 1b show the

DOI: 10.1021/acs.jpcc.9b02244
J. Phys. Chem. C 2019, 123, 9993−9999

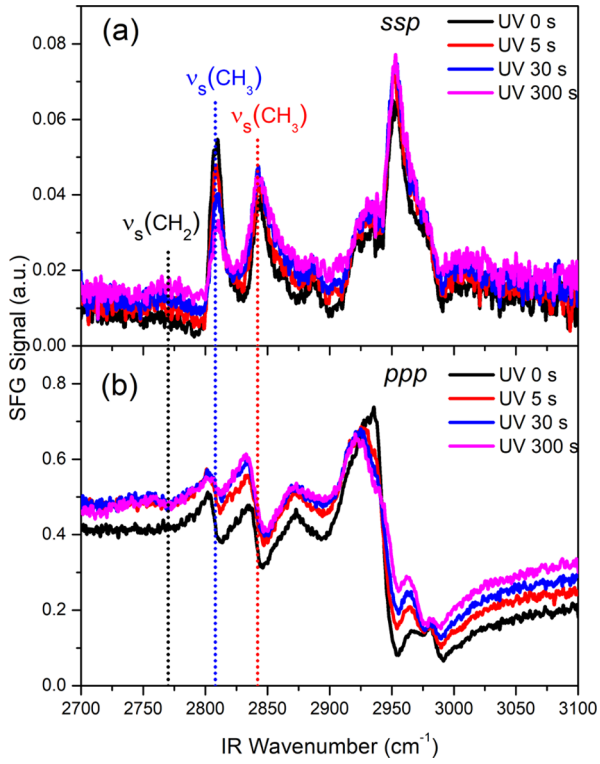

Figure 1. SFG vibrational spectra with ssp (a) and ppp (b) polarization combinations of methanol with one-layer coverage on the TiO_2(110) surface before and after variant UV irradiation times at 400 nm. The substrate was kept at 120 K when the substrate was irradiated by UV and the SFG spectra were taken. Vertical dashed lines indicate the resonant frequencies of methoxy (blue), methanol (red), and formaldehyde (black) on Ti_{5c} sites.

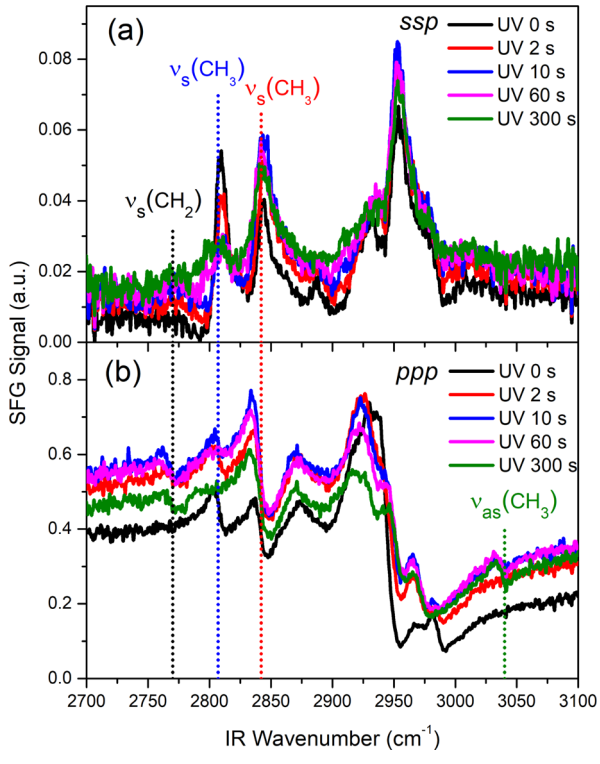

Figure 2. SFG vibrational spectra with ssp (a) and ppp (b) polarization combinations of methanol with one-layer coverage on the TiO_2(110) surface before and after variant UV irradiation times at 400 nm. The substrate was kept at 180 K the substrate was irradiated by UV. The SFG spectra were taken by cooling down the substrate to 120 K. Vertical dashed lines indicate the resonant frequencies of methoxy (blue), methanol (red), formaldehyde (black), and methyl formate (olive) on Ti_{5c} sites.

similar trend as the ssp SFG spectra. However, the ppp SFG spectra after UV irradiation show an additional weak feature at about 2770 cm^{-1} (indicated by black dashed line). The ppp spectra also show the intensity has a small increment, and the peak width is broader at about 2840 cm^{-1}, which is the resonant frequency ν_s of the methyl group from Ti_{5c}−CH_3OH before UV irradiation. Another feature after UV irradiation is that the nonresonance increases with the irradiation time for both ssp and ppp spectra.

Figure 2 shows the SFG vibrational spectra before and after UV irradiation, which are similar as in Figure 1, except that the substrate was kept at 180 K when it was irradiated by UV light. The temperature of 180 K is just about 20 K below the temperature where the first-layer methanol starts desorbing.[8] In Figure 2a, after only 10 s of UV light irradiation, the ν_s feature of methoxy dramatically drops in the ssp spectra, while the intensity of the ν_s feature of methanol turns broader. In Figure 2b, the ppp spectra show much difference after UV irradiation. The ν_s feature of methoxy decreases with the UV irradiation time, while the peak at about 2840 cm^{-1}, assigned to the ν_s of methanol previously, turns broader, and the intensity increases obviously. However, adsorbed methanol should not increase after UV irradiation. There must be some resonance from some new product with similar frequency occasionally. In addition, after only 2 s of UV light irradiation, the ppp spectra show an obviously new feature at around 2770 cm^{-1}. After further 10 s of UV irradiation, this feature continues increasing, the feature at about 2840 cm^{-1} also turns larger notably and another feature at about 3040 cm^{-1} arises. Longer UV irradiation, both features at 2770 and 2840 cm^{-1} decrease and the feature at 3040 cm^{-1} becomes larger. The nonresonance in the ppp spectra shows an increase first and then decreases with the UV irradiation time, while that in the ssp spectra always increases. The increase of the nonresonance might be from the increasing excess electron density induced by surface hydroxyl groups from photocatalytic reactions.[34] However, the different trends of polarization-dependent nonresonance is unclear, which is worth further investigation because of the importance of excess electrons on the surface reactions.[35]

The methanol can be photo-oxidized to formaldehyde and methyl formate stepwise, which has been thoroughly studied.[23−26,36] Based on the spectral assignment of formaldehyde in the gas phase,[37,38] in the condensed phase,[39] and in the adsorbed layer on metals[40] and oxides,[41] we attribute 2770 and 2840 cm^{-1} to the symmetric ($\nu_s(CH_2)$) and antisymmetric ($\nu_{as}(CH_2)$) stretching modes, of CH_2 from formaldehyde, respectively, where the frequency of $\nu_{as}(CH_2)$ is coincident with that of $\nu_s(CH_3)$ of methanol on Ti_{5c}. They are only a little redshift compared with the vibration frequency in the gas phase. This implies that the relating electronic structure of formaldehyde is only weakly perturbed, which is consistent with the theoretical simulation about the $2\pi^*$ state.[42] Based on the infrared spectroscopic studies of methyl formate in the gas phase[43] and on oxides,[44−46] we assign the feature at 3040 cm^{-1} to the antisymmetric stretching mode of CH_3 of methyl formate. This also agrees with the conclusion that the ppp

DOI: 10.1021/acs.jpcc.9b02244
J. Phys. Chem. C 2019, 123, 9993−9999

intensity is always many times that for ssp.[47] Concerning the methyl formate, there should be other two resonant peaks in the range of 2940 to 2970 cm^{-1}, which are the symmetric stretching of CH and CH_3. However, because of the complicated spectral overlapping, it is almost impossible to get the reasonable fitting of these spectra. Hence, we cannot get these resonant frequencies. Table 1 summarizes the spectral assignments of the methanol and the photocatalytic reaction products, formaldehyde and methyl formate, on $TiO_2(110)$ in the C−H stretching range.

Table 1. Assignments of Vibrational Frequencies (cm^{-1}) of Methanol and the Photocatalytic Reaction Products, Formaldehyde and Methyl Formate, on $TiO_2(110)$ in the C−H Stretching Range

		CH_3OH				
assignment[33]		CH_3O-Ti_{5c}		CH_3OH-Ti_{5c}		
$\nu_s(CH_3)$		2806		2841		
		CH_2O				
assignment	$TiO_2(110)$	gas[37,38]	solid[39]	Ag(110)[40]	SiO_2[41]	Al_2O_3[41]
$\nu_s(CH_2)$	2770	2782	2831	2850	2830	2818
$\nu_{as}(CH_2)$	∼2840	2843	2886		2894	2885
		CH_3COOH				
assignment	$TiO_2(110)$	gas[43]		powdered TiO_2[46]	SiO_2[44]	
$\nu_s(CH)$		2943			2952	
$\nu_s(CH_3)$		2969		2960	2964	
$\nu_{as}(CH_3)$	3040	3045		3040	3044	

By comparing the depletion in the ssp spectra under UV irradiation between Figures 1a and 2a, we can find that the photocatalytic reaction for the substrate at 180 K is much more efficient than that for the substrate at 120 K. This temperature dependence of the photocatalytic reaction rate has also been observed before with the low-coverage methanol on $TiO_2(110)$.[24,48] Further, only a little formaldehyde and no methyl formate was produced even after further longer UV irradiation when the substrate was at 120 K. However, when the substrate was at 180 K, we observed not only the production of more formaldehyde but also its depletion and the production of methyl formate. This is consistent with the former reports.[24,25] The only difference between two measurements is the temperature of the substrate when UV shining. The temperature of 180 K is almost the onset of methanol diffusion along the surface Ti_{5c} row from the TPD and STM results.[8,22]

Each step of methanol photooxidation to methoxy, formaldehyde, and further to methyl formate produces the H atom on the O_b site to form OH_b. There is strong repulsion between these OH_b species.[49,50] This repulsion inhibits the new generation of the closed OH_b, which suggests dissociation, and further photo-oxidation of methanol is prevented. As a result, the reaction could be slower and could even stop when the OH_b density is high. However, when the substrate was warmed up and allowed the diffusion of methanol, the newly generated H atom could move apart from the existing OH_b. The OH_b can hop between the different rows of the bridge-bonded O row assisted by the mobile methanol on Ti_{5c} sites,[11] which can also increase the distance between OH_b's and reduce their repulsion. The much diffusive formaldehyde may separate from the OH_b, and close to the methoxy, which can also favor the production of methyl formate.[48,51]

3.2. Methanol Dissociation on Hydroxylated $TiO_2(110)$ Studied by STM. To further determine the effect from the hydroxyl group on the photocatalytic reaction of methanol on $TiO_2(110)$, we carried out the STM studies on methanol dissociation on the hydroxylated surface. Figure 3a−d shows a series of STM images of a single methanol molecule coadsorbed with neighboring OH_b on the $TiO_2(110)$ surface. The partially hydroxylated $TiO_2(110)$ surface was prepared by dosing water on the surface to generate OH_b and then flashing to 400 K to desorb molecular water.[52] STM images are dominated by electronic effects rather than the geometric structure on the $TiO_2(110)$ surface.[53] In Figure 3a−d, the bright rows correspond to low-lying Ti_{5c} atoms, while the dark rows represent topographically high O_b atoms. The faint bright protrusions on the O_b row are oxygen vacancies and the brighter spots on the O_b row are OH_b (marked by dashed circles in Figure 3). Figure 3b1 shows the same area after dosing methanol molecules, and the bright round spot on the Ti_{5c} row can be clearly assigned as a methanol molecule next to OH_b.

After 45 mW laser irradiation for 10 min, Figure 3c1 shows dramatic changes. The bright round spot was changed into a big triangle feature, which looks like consisting of three parts, one big bright spot on the Ti_{5c} row with two faint bright spots on two neighboring O_b row. This feature is very similar to that of single methanol's photodissociation under 355 nm irradiation without OH_b nearby, which is attributed to the formaldehyde molecule on the Ti_{5c} site one step away from the original methanol adsorption site and two OH_b's.[42] With further laser irradiation of 85 mW for 10 min as shown in Figure 3d1, the middle bright spot disappeared, while two spots on different O_b rows remained on the surface. It is noticed that the two spots have different sizes, and the big spot is brighter. After applying a 2 V pulse on the top of the big bright spot (marked by green arrow in Figure 3d1), it was changed into a small spot which resembles the OH_b in Figure 3a1 (see Figure 3e1). Because the H atom of OH_b can be easily removed by voltage above 2 V,[42,54,55] the two bright features in Figure 3c1 are attributed to an OH_b pair[56] on the left and a single OH_b on the right. Hence, the triangle feature in Figure 3c1 consists of a formaldehyde molecule in the middle and three OH_b groups on both O_b rows. In addition, the site where the formaldehyde sits is one Ti_{5c} atom away from the original Ti_{5c} site the methanol adsorbs. This phenomenon is quite different from that of a single methanol on $TiO_2(110)$, that is, both OH_b groups from the photodissociation of a single methanol sit on neighboring O_b sites.[42] Meanwhile, we also observed another condition, as indicated in Figure 3a2−e2. The difference is that the two H atoms from methanol dissociation are on the same O_b row. From the comparison between Figure 3a2,b2, the marked position of OH_b changes by one lattice distance, which could be attributed to the OH_b diffusion mediated by the adsorbed methanol.[11] Hence, it is also possible that OH_b diffuses to the opposite O_b row under UV light irradiation in Figure 3c2,d2.

The dissociation of methanol with neighboring OH_b was observed by STM, while the dissociation possibility is largely different from that on the surface without neighboring OH_b. To further study the OH_b effect on methanol dissociation, qualitative analysis was carried out. During our experiments, after multitime laser irradiation, only 20% (3/15) of the methanol molecules with neighboring OH_b were dissociated, while the dissociation rate without neighboring OH_b is about

DOI: 10.1021/acs.jpcc.9b02244
J. Phys. Chem. C 2019, 123, 9993−9999

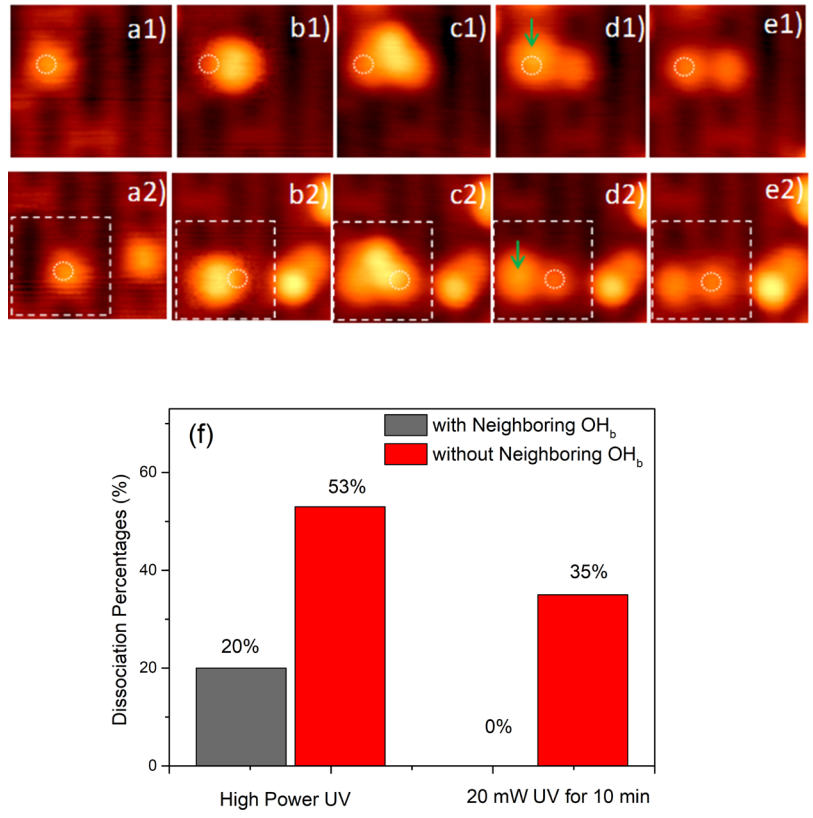

Figure 3. STM images of the photochemical process of methanol molecules with an OH_b on the neighbored BBO site under multiple 355 nm irradiation periods (2.3 nm × 2.3 nm, 1.25 V 100 pA). (a1,a2) Patically hydroxylated TiO_2(110) surface. (b1,b2) Same surface with methanol adsorption which appears as a bright round spot. (c1,c2) In situ images after 45 mW laser irradiation for 15 min. (d1,d2) After another 85 mW laser irradiation for 10 min, an OH_b pair and a single OH_b remained on the surface. (e1,e2) Removal of one H of the OH_b pair by adding 2 V 10 ms pulse on the surface. The dashed rectangles mark the reaction region, and the green arrows and dashed circles represent the positions of adding pulse and OH_bs next to the reactive methanols, respectively. (f) Statistical results of methanol dissociation percentages with and without neighboring OH_b under high-power UV for multi-irradiation (see the main text) and 20 mW for 10 min.

53% (28/53) under the same irradiation condition (the same irradiation power and total duration). Moreover, with the lower UV excitation flux, the difference is larger. After the first-time irradiation of about 20 mW for 10 min, no methanol dissociation was observed with neighboring OH_b, while 35% (19/53) of the methanol molecules without neighboring OH_b were dissociated. It was found that the coexistence of the methoxy on Ti_{5c} and OH_b significantly decreases the yield of formaldehyde because of the reverse reaction from methoxy on Ti_{5c} and OH_b to CH_3OH.[48,57] The additional neighboring OH_b must increase the reverse reaction possibility and lower the photodissociation of methanol.

From the principle of photocatalytic reactions on TiO_2, which is generally accepted,[1] the competition with charge transfer to adsorbed species is mainly the recombination of the electron and hole. Recombination can occur in bulk or on the surface with the release of heat or phonon excitation, which was considered as a detriment to the efficiency of the photocatalyst. However, the conclusion from our experiment results above shows that the thermal motion can enhance the photocatalytic reaction. Intensive UV light, like ultrashort pulsed light, might excite multiple electron and hole pairs in a short time. The massive electron and hole recombination could rapidly generate high excitation of local phonons,[29] which in turn raises the motion and diffusion of adsorbates in tens picosecond scale.[58] Thus, it can increase the photocatalytic reaction. Hence, the recombination of the electron and hole might not have a complete negative effect in photocatalytic reaction processes. From the comparison of results with the high-power and the lower-power UV irradiation in STM experiments above and the high-intensive UV light[23] and low-intensive continuous wave light[21] in the literature, the high-intensive UV light could dramatically enhance the quantum yield of photocatalytic reactions. High-energy charge carriers can be generated by photons, which are larger than the band gap. These charge carriers in TiO_2 rapidly thermalize to their respective band edges because of carrier−carrier and carrier−phonon scatterings, and local phonons can be excited in the meantime. These excited phonons, or the local heat, can promote the movement and mobility of the adsorbate and then increase the photocatalytic reaction. This could be another possible mechanism to explain the strong photon energy dependence of the photocatalytic dissociation rate of methanol on TiO_2(110), which has been observed.[29]

4. CONCLUSIONS

In summary, we used surface SFG-VS in the C−H stretching range to in situ identify the photocatalytic products, formaldehyde and methyl formate, of methanol on TiO_2(110). This provides the vibrational assignment information for future possible time-resolved experiments on the photocatalytic reaction dynamics. We also observed the temperature dependence of photocatalytic reaction and proposed that the diffusion of adsorbates limits the further photocatalytic

DOI: 10.1021/acs.jpcc.9b02244
J. Phys. Chem. C 2019, 123, 9993−9999

reaction because of the repulsion from OH_b. Further evidence of the inhibition of photocatalytic reactions from OH_b was provided by STM experiments combined with UV light on the photodissociation of methanol on the hydroxylated TiO_2(110) surface. This work provides detailed insights into the photo-oxidation of methanol on TiO_2(110) and help better understand the photochemistry of organic molecules on oxides at the molecular level.

AUTHOR INFORMATION

Corresponding Authors

*E-mail: zhbma@dicp.ac.cn (Z.M.).
*E-mail: zfren@dicp.ac.cn (Z.R.).

ORCID

Haochen Wang: 0000-0003-0234-7932
Qing Guo: 0000-0003-0265-1184
Chuanyao Zhou: 0000-0002-3252-2992
Zefeng Ren: 0000-0002-5263-9346

Author Contributions

⊥R.Z. and H.W. contributed equally to this work.

Notes

The authors declare no competing financial interest.

ACKNOWLEDGMENTS

This work was supported by the Ministry of Science and Technology (grant nos. 2018YFA0208700 and 2016YFA0200602), Chinese Academy of Sciences (grant no. XDB17000000), National Natural Science Foundation of China (grant nos. 91645125, 21673236 and 21688102), and the Youth Innovation Promotion Association of CAS under grant no. 2017224.

REFERENCES

(1) Linsebigler, A. L.; Lu, G.; Yates, J. T. Photocatalysis on TiO_2 Surfaces: Principles, Mechanisms, and Selected Results. *Chem. Rev.* **1995**, *95*, 735−758.
(2) Thompson, T. L.; Yates, J. T. Surface science studies of the photoactivation of TiO_2-new photochemical processes. *Chem. Rev.* **2006**, *106*, 4428−4453.
(3) Dohnálek, Z.; Lyubinetsky, I.; Rousseau, R. Thermally-driven Processes on Rutile TiO_2(110)-(1×1): A Direct View at the Atomic Scale. *Prog. Surf. Sci.* **2010**, *85*, 161−205.
(4) Chen, H.; Nanayakkara, C. E.; Grassian, V. H. Titanium Dioxide Photocatalysis in Atmospheric Chemistry. *Chem. Rev.* **2012**, *112*, 5919−5948.
(5) Henderson, M. A.; Lyubinetsky, I. Molecular-Level Insights into Photocatalysis from Scanning Probe Microscopy Studies on TiO_2(110). *Chem. Rev.* **2013**, *113*, 4428−4455.
(6) Guo, Q.; Zhou, C.; Ma, Z.; Ren, Z.; Fan, H.; Yang, X. Elementary photocatalytic chemistry on TiO_2 surfaces. *Chem. Soc. Rev.* **2016**, *45*, 3701−3730.
(7) Guo, Q.; Zhou, C.; Ma, Z.; Ren, Z.; Fan, H.; Yang, X. Elementary Chemical Reactions in Surface Photocatalysis. *Annu. Rev. Phys. Chem.* **2018**, *69*, 451−472.
(8) Henderson, M. A.; Otero-Tapia, S.; Castro, M. E. The Chemistry of Methanol on the TiO_2(110) Surface: the Influence of Vacancies and Coadsorbed Species. *Faraday Discuss.* **1999**, *114*, 313−329.
(9) Farfan-Arribas, E.; Madix, R. J. Role of Defects in the Adsorption of Aliphatic Alcohols on the TiO_2(110) Surface. *J. Phys. Chem. B* **2002**, *106*, 10680−10692.
(10) Farfan-Arribas, E.; Madix, R. J. Different binding sites for methanol dehydrogenation and deoxygenation on stoichiometric and defective TiO_2(110) surfaces. *Surf. Sci.* **2003**, *544*, 241−260.
(11) Zhang, Z.; Bondarchuk, O.; White, J. M.; Kay, B. D.; Dohnálek, Z. Imaging Adsorbate O-H Bond Cleavage: Methanol on TiO_2(110). *J. Am. Chem. Soc.* **2006**, *128*, 4198−4199.
(12) de Armas, R. S.; Oviedo, J.; San Miguel, M. A.; Sanz, J. F. Methanol adsorption and dissociation on TiO_2(110) from first principles calculations. *J. Phys. Chem. C* **2007**, *111*, 10023−10028.
(13) Zhao, J.; Yang, J.; Petek, H. Theoretical study of the molecular and electronic structure of methanol on a TiO_2(110) surface. *Phys. Rev. B: Condens. Matter Mater. Phys.* **2009**, *80*, 235416.
(14) Zhou, C.; Ren, Z.; Tan, S.; Ma, Z.; Mao, X.; Dai, D.; Fan, H.; Yang, X.; LaRue, J.; Cooper, R.; Wodtke, A. M.; Wang, Z.; Li, Z.; Wang, B.; Yang, J.; Hou, J. Site-specific Photocatalytic Splitting of Methanol on TiO_2(110). *Chem. Sci.* **2010**, *1*, 575−580.
(15) Sánchez, V. M.; Cojulun, J. A.; Scherlis, D. A. Dissociation Free Energy Profiles for Water and Methanol on TiO_2 Surfaces. *J. Phys. Chem. C* **2010**, *114*, 11522−11526.
(16) Bates, S. P.; Gillan, M. J.; Kresse, G. Adsorption of Methanol on TiO_2(110): A First-Principles Investigation. *J. Phys. Chem. B* **1998**, *102*, 2017−2026.
(17) Kawai, T.; Sakata, T. Photocatalytic hydrogen production from liquid methanol and water. *J. Chem. Soc., Chem. Commun.* **1980**, *15*, 694−695.
(18) Kawai, M.; Naito, S.; Tamaru, K.; Kawai, T. The mechanism of photocatalytic hydrogen production from gaseous methanol and water: IR spectroscopic approach. *Chem. Phys. Lett.* **1983**, *98*, 377−380.
(19) Harada, H.; Ueda, T. Photocatalytic activity of ultra-fine rutile in methanol-water solution and dependence of activity on particle size. *Chem. Phys. Lett.* **1984**, *106*, 229−231.
(20) Al-Mazroai, L. S.; Bowker, M.; Davies, P.; Dickinson, A.; Greaves, J.; James, D.; Millard, L. The photocatalytic reforming of methanol. *Catal. Today* **2007**, *122*, 46−50.
(21) Shen, M.; Henderson, M. A. Identification of the Active Species in Photochemical Hole Scavenging Reactions of Methanol on TiO_2. *J. Phys. Chem. Lett.* **2011**, *2*, 2707−2710.
(22) Shen, M.; Acharya, D. P.; Dohnálek, Z.; Henderson, M. A. Importance of Diffusion in Methanol Photochemistry on TiO2(110). *J. Phys. Chem. C* **2012**, *116*, 25465−25469.
(23) Guo, Q.; Xu, C.; Ren, Z.; Yang, W.; Ma, Z.; Dai, D.; Fan, H.; Minton, T. K.; Yang, X. Stepwise Photocatalytic Dissociation of Methanol and Water on TiO_2(110). *J. Am. Chem. Soc.* **2012**, *134*, 13366−13373.
(24) Guo, Q.; Xu, C.; Yang, W.; Ren, Z.; Ma, Z.; Dai, D.; Minton, T. K.; Yang, X. Methyl Formate Production on TiO_2(110), Initiated by Methanol Photocatalysis at 400 nm. *J. Phys. Chem. C* **2013**, *117*, 5293−5300.
(25) Yuan, Q.; Wu, Z.; Jin, Y.; Xu, L.; Xiong, F.; Ma, Y.; Huang, W. Photocatalytic Cross-Coupling of Methanol and Formaldehyde on a Rutile TiO_2(110) Surface. *J. Am. Chem. Soc.* **2013**, *135*, 5212−5219.
(26) Phillips, K. R.; Jensen, S. C.; Baron, M.; Li, S.-C.; Friend, C. M. Sequential Photo-oxidation of Methanol to Methyl Formate on TiO_2(110). *J. Am. Chem. Soc.* **2012**, *135*, 574−577.
(27) Xu, C.; Yang, W.; Guo, Q.; Dai, D.; Chen, M.; Yang, X. Molecular Hydrogen Formation from Photocatalysis of Methanol on TiO_2(110). *J. Am. Chem. Soc.* **2013**, *135*, 10206−10209.
(28) Liu, S.; Liu, A.-a.; Wen, B.; Zhang, R.; Zhou, C.; Liu, L.-M.; Ren, Z. Coverage Dependence of Methanol Dissociation on TiO_2(110). *J. Phys. Chem. Lett.* **2015**, *6*, 3327−3334.
(29) Xu, C.; Yang, W.; Ren, Z.; Dai, D.; Guo, Q.; Minton, T. K.; Yang, X. Strong Photon Energy Dependence of the Photocatalytic Dissociation Rate of Methanol on TiO_2(110). *J. Am. Chem. Soc.* **2013**, *135*, 19039−19045.
(30) Chabal, Y. J. Surface infrared spectroscopy. *Surf. Sci. Rep.* **1988**, *8*, 211−357.
(31) Wang, Y.; Wöll, C. Chemical reactions on metal oxide surfaces investigated by vibrational spectroscopy. *Surf. Sci.* **2009**, *603*, 1589−1599.
(32) Liu, S.; Liu, A.-a.; Zhang, R.; Ren, Z. Compact ultrahigh vacuum/high-pressure system for broadband infrared sum frequency

DOI: 10.1021/acs.jpcc.9b02244
J. Phys. Chem. C 2019, 123, 9993−9999

generation vibrational spectroscopy studies. *Rev. Sci. Instrum.* **2016**, *87*, 044101.
(33) Liu, A.-a.; Liu, S.; Zhang, R.; Ren, Z. Spectral Identification of Methanol on TiO_2(110) Surfaces with Sum Frequency Generation in the C−H Stretching Region. *J. Phys. Chem. C* **2015**, *119*, 23486−23494.
(34) Feng, R.-r.; Liu, A.-a.; Liu, S.; Shi, J.; Zhang, R.; Ren, Z. In Situ Studies on the Dissociation and Photocatalytic Reactions of CH_3OH on TiO_2 Thin Film by Sum Frequency Generation Vibrational Spectroscopy. *J. Phys. Chem. C* **2015**, *119*, 9798−9804.
(35) Pang, C. L.; Lindsay, R.; Thornton, G. Chemical reactions on rutile TiO_2(110). *Chem. Soc. Rev.* **2008**, *37*, 2328−2353.
(36) Wei, D.; Jin, X.; Huang, C.; Dai, D.; Ma, Z.; Li, W.-X.; Yang, X. Direct Imaging Single Methanol Molecule Photocatalysis on Titania. *J. Phys. Chem. C* **2015**, *119*, 17748−17754.
(37) Khoshkhoo, H.; Nixon, E. R. Infrared and Raman spectra of formaldehyde in argon and nitrogen matrices. *Spectrochim. Acta, Part A* **1973**, *29*, 603−612.
(38) Brown, L. R.; Hunt, R. H.; Pine, A. S. Wavenumbers, line strengths, and assignments in the Doppler-limited spectrum of formaldehyde from 2700 to 3000 cm^{-1}. *J. Mol. Spectrosc.* **1979**, *75*, 406−428.
(39) Khoshkoo, H.; Hemple, S. J.; Nixon, E. R. Infrared and Raman studies of solid formaldehyde. *Spectrochim. Acta, Part A* **1974**, *30*, 863−868.
(40) Stuve, E. M.; Madix, R. J.; Sexton, B. A. An EELS study of the oxidation of H_2CO on Ag(110). *Surf. Sci.* **1982**, *119*, 279−290.
(41) Busca, G.; Lamotte, J.; Lavalley, J. C.; Lorenzelli, V. FT-IR study of the adsorption and transformation of formaldehyde on oxide surfaces. *J. Am. Chem. Soc.* **1987**, *109*, 5197−5202.
(42) Wei, D.; Jin, X.; Huang, C.; Dai, D.; Ma, Z.; Li, W.-X.; Yang, X. Direct Imaging Single Methanol Molecule Photocatalysis on Titania. *J. Phys. Chem. C* **2015**, *119*, 17748−17754.
(43) Shimanouchi, T. *Tables of Molecular Vibrational Frequencies Consolidated*; National Bureau of Standards, 1972; Vol. *I*.
(44) Millar, G. J.; Rochester, C. H.; Waugh, K. C. Infrared study of methyl formate and formaldehyde adsorption on reduced and oxidised silica-supported copper catalysts. *J. Chem. Soc., Faraday Trans.* **1991**, *87*, 2785−2793.
(45) Millar, G. J.; Rochester, C. H.; Waugh, K. C. Evidence for the Adsorption of Molecules at Special Sites Located at Copper-Zinc Oxide Interfaces. *J. Chem. Soc., Faraday Trans.* **1992**, *88*, 3497−3503.
(46) Chuang, C.-C.; Wu, W.-C.; Huang, M.-C.; Huang, I.-C.; Lin, J.-L. FTIR study of adsorption and reactions of methyl formate on powdered TiO_2. *J. Catal.* **1999**, *185*, 423−434.
(47) Wang, H.-F.; Gan, W.; Lu, R.; Rao, Y.; Wu, B.-H. Quantitative spectral and orientational analysis in surface sum frequency generation vibrational spectroscopy (SFG-VS). *Int. Rev. Phys. Chem.* **2005**, *24*, 191−256.
(48) Feng, H.; Tan, S.; Tang, H.; Zheng, Q.; Shi, Y.; Cui, X.; Shao, X.; Zhao, A.; Zhao, J.; Wang, B. Temperature- and Coverage-Dependent Kinetics of Photocatalytic Reaction of Methanol on TiO_2(110)-(1 x 1) Surface. *J. Phys. Chem. C* **2016**, *120*, 5503−5514.
(49) Li, S.-C.; Zhang, Z.; Sheppard, D.; Kay, B. D.; White, J. M.; Du, Y.; Lyubinetsky, I.; Henkelman, G.; Dohnálek, Z. Intrinsic Diffusion of Hydrogen on Rutile TiO_2(110). *J. Am. Chem. Soc.* **2008**, *130*, 9080−9088.
(50) Du, Y.; Petrik, N. G.; Deskins, N. A.; Wang, Z.; Henderson, M. A.; Kimmel, G. A.; Lyubinetsky, I. Hydrogen reactivity on highly-hydroxylated TiO_2(110) surfaces prepared via carboxylic acid adsorption and photolysis. *Phys. Chem. Chem. Phys.* **2012**, *14*, 3066−3074.
(51) Lang, X.; Wen, B.; Zhou, C.; Ren, Z.; Liu, L.-M. First-Principles Study of Methanol Oxidation into Methyl Formate on Rutile TiO_2(110). *J. Phys. Chem. C* **2014**, *118*, 19859−19868.
(52) Wendt, S.; Schaub, R.; Matthiesen, J.; Vestergaard, E. K.; Wahlström, E.; Rasmussen, M. D.; Thostrup, P.; Molina, L. M.; Lægsgaard, E.; Stensgaard, I.; Hammer, B.; Besenbacher, F. Oxygen vacancies on TiO_2(110) and their interaction with H_2O and O_2: A combined high-resolution STM and DFT study. *Surf. Sci.* **2005**, *598*, 226−245.
(53) Diebold, U.; Anderson, J. F.; Ng, K.-O.; Vanderbilt, D. Evidence for the Tunneling Site on Transition-Metal Oxides: TiO_2(110). *Phys. Rev. Lett.* **1996**, *77*, 1322−1325.
(54) Zhang, Z.; Bondarchuk, O.; Kay, B. D.; White, J. M.; Dohnálek, Z. Imaging water dissociation on TiO_2(110): Evidence for inequivalent geminate OH groups. *J. Phys. Chem. B* **2006**, *110*, 21840−21845.
(55) Bikondoa, O.; Pang, C. L.; Ithnin, R.; Muryn, C. A.; Onishi, H.; Thornton, G. Direct visualization of defect-mediated dissociation of water on TiO_2(110). *Nat. Mater.* **2006**, *5*, 189−192.
(56) Cui, X.; Wang, Z.; Tan, S.; Wang, B.; Yang, J.; Hou, J. G. Identifying Hydroxyls on the TiO_2(110)-1 x 1 Surface with Scanning Tunneling Microscopy. *J. Phys. Chem. C* **2009**, *113*, 13204−13208.
(57) Mao, X.; Wei, D.; Wang, Z.; Jin, X.; Hao, Q.; Ren, Z.; Dai, D.; Ma, Z.; Zhou, C.; Yang, X. Recombination of Formaldehyde and Hydrogen Atoms on TiO_2(110). *J. Phys. Chem. C* **2015**, *119*, 1170−1174.
(58) Frischkorn, C.; Wolf, M. Femtochemistry at metal surfaces: Nonadiabatic reaction dynamics. *Chem. Rev.* **2006**, *106*, 4207−4233.

DOI: 10.1021/acs.jpcc.9b02244
J. Phys. Chem. C 2019, 123, 9993−9999